Combined NMR and Quantum Chemical Studies on the Interaction between Trehalose and Dienes Relevant to the Antioxidant Function of Trehalose

Kazuyuki Oku,[†] Mayumi Kurose,[†] Michio Kubota,[†] Shigeharu Fukuda,[†] Masashi Kurimoto,[†] Yoshio Tujisaka,[†] Atsutoshi Okabe,[‡] and Minoru Sakurai*[,‡]

Amase Institute, Hayashibara Biochemical Laboratories, Inc., 7-7 Amaseminami-machi, Okayama 700-0834, Japan, and Center for Biological Resources and Informatics, Tokyo Institute of Technology, B-62 4259 Nagatsuta-cho, Midori-ku, Yokohama 226-8501, Japan

Received: September 10, 2004; In Final Form: November 15, 2004

In a previous study (Oku, K.; Watanabe, H.; Kubota, M.; Fukuda, S.; Kurimoto, M.; Tujisaka, Y.; Komori, M.; Inoue, Y.; Sakurai, M. *J. Am. Chem. Soc.* **2003**, *125*, 12739), we investigated the mechanism of the antioxidant function of trehalose against unsaturated fatty acids (UFAs) and revealed that the key factor relevant to the function is the formation of OH···π and CH···O hydrogen bonds between trehalose and the cis double bonds of the UFA. Here, we investigate whether such intriguing interactions also occur between this sugar and cis double bonds in other unsaturated compounds. For this purpose, we selected various diene compounds (1,3-butadiene, 1,3-pentadiene, 1,4-pentadiene, and 2,5-heptadiene) as interaction partners. All NMR experiments performed, including ^{1}H−^{1}H NOESY measurements, indicated that trehalose selectively interacts with the *cis*-olefin proton pair in the above diene with a 1:1 stoichiometry, and the C-3 (C-3′) and C-6′ (C-6) sites of the sugar are responsible for the interaction. Similar interactions were not observed for the mixtures of the diene and other saccharides (neotrehalose, kojibiose, nigerose, maltose, isomaltose, sucrose, maltitol, and sorbitol). Quantum chemical calculations revealed that the OH-3 and OH-6 groups bind to the olefin double bonds of the diene through OH···π and CH···O types of hydrogen bonds, respectively, and the stabilization energy of the resulting complex is 5−6 kcal mol^{-1}. These results strongly support the above NMR results. Finally, the activation energies were calculated for the hydrogen abstraction reactions from the activated methylene group of heptadiene. In particular, when the reaction was initiated by a methyl radical, the activation energy was only 10 kcal mol^{-1} for the free heptadiene, but on complexation with trehalose it drastically increased to ca. 40 kcal mol^{-1}. This indicates that trehalose has a significant depression effect on the oxidation of the diene compounds. These results strongly support the antioxidant mechanism deduced in the previous study and indicate that the formation of unique multiple hydrogen bonds between trehalose and *cis*-olefin bonds is rather a general event not confined to the case of UFA.

Introduction

Trehalose is a nonreducing disaccharide consisting of two D-glucose molecules linked together by an α,α-1,1-linkage. This saccharide occurs widely in nature, microorganisms, plants, and invertebrates.[1] Recently, a mass production of trehalose from starch was developed, and this saccharide is extensively used in the food, cosmetic, pharmaceutical, and medicinal industries.[2,3] Trehalose is well-known to act as a protectant against various stresses,[4−9] such as desiccation, heat, freezing, or osmotic shock. Thus, this saccharide is frequently utilized in the preservation of ingredients of food, starch, protein, and so on. In addition to the protection function against water stresses, there is growing evidence that trehalose acts as an antioxidant. Lipid peroxidation is a critical factor leading to deterioration in lipid-containing foods during processing, transportation, and storage.[10] Thus, it is of great interest to improve the oxidative stability of lipid-containing foods. Recently, we reported that trehalose effectively depresses the heat- or radical-induced peroxidation of unsaturated fatty acids (UFAs).[11,12] In addition, the antioxidant function of this sugar was also demonstrated from an in vivo study of yeast cells, in which the protection of the cellular proteins from damage by oxygen radicals was investigated in detail.[13]

In general, the oxidation of an UFA is initiated by the so-called autoxidation reaction, in which activated oxygen or free radicals attract hydrogen atoms from the allyl group of the UFA.[14,15] In the subsequent promotion reaction, the resultant conjugated diene reacts with O_2 and another UFA molecule to produce a hydroperoxy fatty acid, which undergoes degradation or polymerization by the secondary oxidation reaction.[10] Our study showed that trehalose greatly depresses the reaction rate of the autoxidation step rather than those of the subsequent reactions.[12] In addition, other disaccharides, such as sucrose, maltose, and neotrehalose, exhibited no apparent effect on this step. It seems that the antioxidant function of trehalose is due to neither the radical-scavenger nor metal-sequestration function.[11,12] Thus, elucidation of the antioxidant mechanism of trehalose is a highly challenging issue in carbohydrate chemistry.

Most recently, we investigated the mechanism of the antioxidant function of trehalose against an UFA from experimental and theoretical viewpoints. In that study[16] (hereafter called paper 1), NMR experiments indicated that trehalose forms intermo-

* Author to whom correspondence should be addressed. Phone: (+81) 45-924-5795. Fax: (+81) 45-924-5827. E-mail: msakurai@bio.titech.ac.jp.
[†] Hayashibara Biochemical Laboratories, Inc.
[‡] Tokyo Institute of Technology.

10.1021/jp045906w CCC: $30.25
Published on Web 01/22/2005

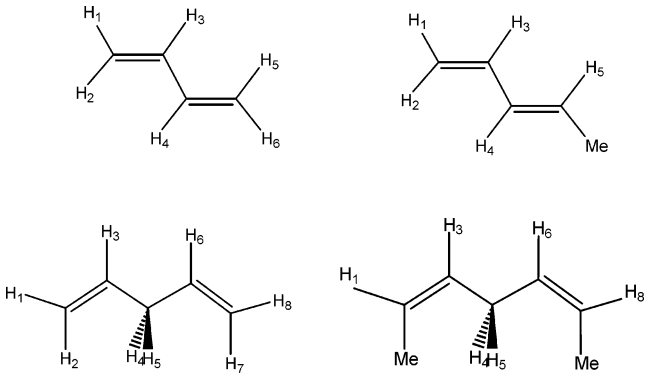

Figure 1. Numbering of the hydrogen atoms in the diene compounds studied.

lecular complexes with UFAs possessing *cis*-olefin double bonds, such as linoleic acid and α-linolenic acid, and the OH-3 and OH-6 groups of the sugar are responsible for the interaction. Quantum chemical calculations suggested that such a complex is stabilized through the formation of OH···π and CH···O hydrogen bonds between trehalose and the cis double bonds of the UFA. Furthermore, it was revealed that the formation of such a multiple hydrogen bond causes a significant increase in the activation energy for hydrogen abstraction reaction from the activated methylene group interposed between two double bonds and hence leads to a significant depression effect on the oxidation of the UFA. Thus, paper 1 successfully accounted for the molecular mechanism of the antioxidant function of trehalose.

However, we think that the following issues should be investigated in more detail. First, it remains unclear whether the above multiple hydrogen bond occurs exclusively between trehalose and the cis double bonds in the UFA, in other words, whether the interaction is more general of events that also occur between trehalose and other cis double bonds. Second, in paper 1, there was a minor discrepancy between the NMR results and the quantum chemical computational results. Namely, while the experiments identified the OH-3 and OH-6′ groups as the interaction sites with the UFA, the computational model obtained suggested that the OH-2 and the OH-6′ groups participated in the interaction. Here, we attempt to search for intermolecular interaction models completely consistent with the experimental facts. Third, in paper 1, the activation energy calculations were applied to a simple hydrogen abstraction reaction from the activate methylene group. However, under usual experimental conditions, the reaction is initiated by free radicals generated by various environmental stimulations such as heat, light, and metals. Thus, it is necessary to study more realistic reactions in which the effect of the free radical is explicitly taken into account.

In this study, to address the above first issue, we investigate the interaction of trehalose with various diene compounds (1,3 butadiene, 1,3-pentadiene, 1,4-pentadiene, and 2,5-heptadiene; Figure 1). On the basis of the results from ^{1}H and ^{13}C spin−lattice relaxation time (T_1) and ^{1}H−^{1}H NOESY measurements, it will be shown that trehalose selectively interacts with the *cis*-olefin double bonds of these diene compounds. In addition, it is shown that other saccharides (neotrehalose, kojibiose, nigerose, maltose, isomaltose, sucrose, maltitol, and sorbitol) do not share such a property. The second issue is successfully solved by careful quantum chemical calculations, which provide the interaction model in which the OH-3 and OH-6′ groups of trehalose are binding to a *cis*-olefin double bond. Finally, to address the third issue, we investigate the hydrogen abstraction reaction initiated by a methyl radical and again find a significant depression effect of trehalose on the oxidation of the diene. The present results strongly support the antioxidant mechanism deduced in the previous study and indicate the universality of the unique hydrogen bond formation between trehalose and *cis*-olefin bonds.

Materials and Methods

Chemicals. Trehalose (>99.9% purity), neotrehalose (α-D-glucopyranosyl β-D-glucopyranoside, 99.8%), nigerose (2-O-α-D-glucopyranosyl-D-glucose, 97.0%), kojibiose (3-O-α-D-glucopyranosyl-D-glucose, 98.0%), maltose (4-O-α-D-glucopyranosyl-D-glucose, 99.9%), isomaltose (6-O-α-D-glucopyranosyl-D-glucose, 99.9%), and maltitol (4-O-α-D-glucopyranosyl-D-sorbitol, 99.3%) were produced by Hayashibara Biochemical Laboratories, Inc., Okayama, Japan. Sucrose (α-D-glucopyranosyl β-D-fructofuranoside, >99%) and sorbitol (D-sorbitol, >99%) were purchased from Wako Pure Chemical Industries, Osaka, Japan and Tokyo Chemical Industries Co., Tokyo, Japan, respectively.

1,3-Butadiene (>99%) was purchased from Tokyo Chemical Industry Co. All *cis*-1,3-pentadiene (>99%), *cis*,*trans*-1,3-pentadiene (>98.0%), 1,4-pentadiene (>98%), and all *cis*-2,5-heptadiene (>95%) were obtained from Wako Pure Chemical Industries.

NMR Experiments. The samples for NMR experiments were prepared as follows. First, we separately prepared a solution of diene and several solutions of trehalose with different concentrations. In the case of the diene, the former consists of 10 mg of the diene and 0.9 mL of methanol-d_4 (D, 99.8%, Cambridge Isotope Laboratories, MA), and the latter contains 0 to 48.2 mg of trehalose dihydrate and 0.1 mL of deuterium oxide (D, 99.9%, Cambridge Isotope Laboratories, MA). By mixing these solutions, we obtained NMR samples with integer molar ratios between diene and trehalose. The NMR measurements were done at 25 °C by using an FT-NMR spectrometer (model JMN-AL300, Nihon Denshi Co. Tokyo, Japan), operating at 300.4 MHz (^{1}H frequency) or 75.45 MHz (^{13}C frequency). The ^{1}H or ^{13}C chemical shifts (δ) were measured with respect to the ^{1}H or ^{13}C signals of tetramethylsilane (Wako Pure Chemical Industries) dissolved in the samples, respectively. The spin−lattice relaxation times of ^{1}H and ^{13}C (hereafter abbreviated as ^{1}H−T_1 and ^{13}C−T_1, respectively) were measured using a conventional inversion−recovery pulse sequence, that is, a repeated 90°−τ −90° pulse. The repetition time was taken to be always 5 times greater than T_1. For both ^{1}H−T_1 and ^{13}C−T_1, the signal recovery was single-exponential decay. The ^{1}H−T_1 measurements were performed for major ^{1}H peaks assigned to the diene. ^{1}H−^{1}H NOESY spectra were obtained for the mixture of trehalose and 1,4-pentadiene (molar ratio of 2:1). NOE measurements were performed using the pulse sequence depicted below

$$^1\text{H: } 90-t_1-90-\tau_m-90-\text{ACQTM}-$$

where the mixing time τ_m was taken to be 5 s and the acquisition time ACQTM was taken to be 2.7 s. The NMR data were processed by using a software package, Alice WINNMR 2.1, attached to the NMR apparatus.

Calculations. The interactions between trehalose and the diene compounds were examined using several model systems, including trehalose/2-butene, trehalose/heptadiene, and methanol/heptadiene complexes. The initial structures of all of the models were obtained by the MM2 force field calculations, using the

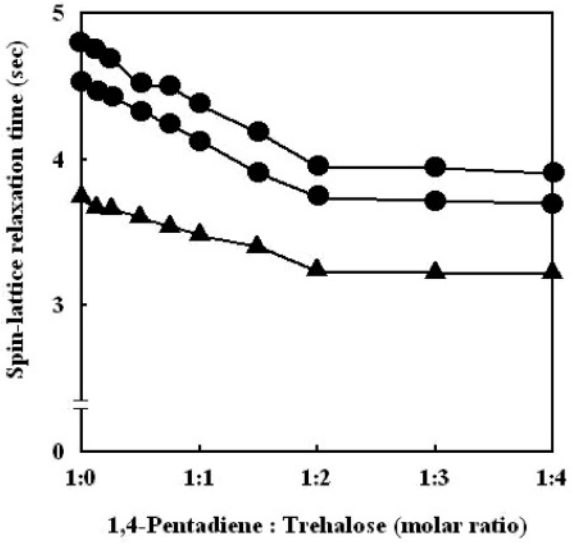

Figure 2. Effect of molar ratio of trehalose to 1,4-pentadiene on the T_1 relaxation times of the olefin and the activated methylene protons: ●, H-1,3,6,8 (olefin proton); ▲, H-4,5 (activated methylene proton).

ChemOffice Ultra program (Cambridge Scientific Computing).[17] Those structures were first optimized by semiempirical PM3 calculations, using the MOPAC 2000 program.[18] And the resulting structures were further optimized by ab inito Harteree−Fock (HF) or density functional theory (DFT) calculations, using the Gaussian 98 program.[19] The HF and DFT optimization calculations were carried out at the HF/6-31G** and B3LYP/6-31G** levels of theory, respectively, and the interaction energies of trehalose with the diene compounds were obtained at the same levels. To examine the effects of electron correlation and basis set superposition error on the interaction energies, higher levels of theory were applied to the trehalose/2-butene complex, namely, HF/6-311++G**//HF/6-31G**, MP2/6-31G**//HF/6-31G**, and B3LYP/6-311++G**//B3LYP/6-31G**. The search for the transition state in the hydrogen abstraction reaction was carried out according to a standard protocol, using the UHF/6-31G** and UB3LYP/6-31G** methods.

Results

NMR Analysis for the Trehalose/Diene Complexation. First, we measured the effect of trehalose on the spin−lattice relaxation times of the proton signals (^{1}H−T_1) of the dienes. Figure 2 shows the dependence of the ^{1}H−T_1 values of the olefin (H-1,3,6,8) and the activated methylene protons (H-4,5) of 1,4-pentadiene on the trehalose concentration. The these ^{1}H−T_1 values decrease with an increase in trehalose concentration, and all of the curves reach a plateau at a 2:1 molar ratio of trehalose to 1,4-pentadiene. Such characteristic T_1 changes were not observed for the H-2 and H-7 signals. The present NMR measurements were carried out under the so-called extremely narrowing conditions: the decrease of the T_1 value signifies a decrease in the mobility of a molecule or molecular fragment of interest.[20] Thus, it is inferred that the T_1 changes shown in Figure 2 are caused by the formation of an intermolecular complex between trehalose and the diene, because the binding of trehalose could lower the mobility of the diene. In addition, Figure 2 suggests that such complexation occurs with a 2:1 stoichiometry between the sugar and the diene. The olefin protons (H-1,3,6,8) that exhibited the characteristic T_1 changes have a common structural property; that is to say, H-1 and H-3 (or H-6 and H-8) are positioned on the same side with respect to the C1═C2 double bond (C4═C5 double bond). This implies that the intermolecular interactions responsible for the complexation selectively occur at the *cis*-olefin hydrogen pairs rather than the trans-type ones (H-2 and -3, and H-4 and -5).

TABLE 1: Effect of Trehalose on the Spin−Lattice Relaxation Time (T_1) of 1,4-Pentadiene

		spin−lattice relaxation time T_1/s[a]	
	chemical shifts/ppm	without trehalose	with trehalose
H-3,6	5.49	4.80	3.95
	5.82	4.71	3.72
H-2,7	5.06	4.06	4.15
	5.06	4.40	4.21
	4.99	4.61	4.47
	4.99	4.54	4.42
H-1,8	5.01	4.53	3.74
H-4,5	2.79	3.73	3.23
	2.78	3.69	3.05

[a] The T_1 measurements were performed at the molar ratio of trehalose/1,4-pentadiene = 2:1.

Table 1 summarizes the data for the 2:1 mixture of trehalose with other diene compounds (1,3-butadiene, 1,3-pentadiene, and 2,5-heptadiene). 1,3-Butadiene has two sets of cis-type hydrogen pairs (H-1 and -3 and H-4 and -6) and two sets of the trans-type ones (H-2 and -3 and H-4 and -5), and the T_1 values for the former protons alone exhibited significant changes. Similarly, in 1,3-pentadiene, the cis-proton pair (H-1 and -3) exhibited T_1 changes by addition of trehalose. 1,3-Pentadiene and 2,5-heptadiene have trans and cis C═C double bonds, respectively. While no apparent T_1 changes were observed for the trans-type proton pair (H-4 and -5) in the former diene, all of the cis-proton pairs in the latter exhibited significant T_1 changes. Through combination of these results, it can be safely said that trehalose can interact only with the cis double bond (or *cis*-olefin hydrogen pair) in the diene.

The results for other saccharides (neotrehalose, nigerose, kojibiose, maltose, isomaltose, sucrose, maltitol, and sorbitol) are also summarized in Table 1, where all of the ^{1}H−T_1 measurements were performed at the molar ratio of sugar/diene = 2:1. These sugars exerted no apparent effect on the T_1 values of all of the proton signals of the partner diene. Therefore, it is concluded that the complex formation with a diene is a unique phenomenon to trehalose.

The T_1 measurements of ^{13}C nuclei (^{13}C−T_1) for trehalose/diene mixtures supported the above ^{1}H−T_1 results. Table 2 shows the results for the mixture of trehalose/1,4-pentadiene = 2:1. In the absence of trehalose, the T_1 values of the C-1,5 and C-2,4 carbon nuclei were 7.19 and 6.76 s for C-1,5 and C-2,4, respectively, and after addition of the sugar they decreased to 5.79 and 5.99 s. The ^{13}C−T_1 value of the activated methylene carbon, C-3 in 1,4-pentadiene, exhibited no apparent change by addition of trehalose, although the T_1 values of the corresponding methylene protons were significantly influenced by the sugar (Table 1). In general, the ^{1}H−T_1 value is dependent on both the intra- and intermolecular dipole−dipole relaxation processes. It is thought that the ^{1}H−T_1 process of the activated methylene protons might be modulated by the intermolecular dipole−dipole interactions with protons of the trehalose bound to the neighboring double bonds.[21] Through combination of the ^{1}H−T_1 and ^{13}C−T_1 results, it is reasonable to interpret that the sites of the diene directly interacting with trehalose are the C═C double bonds rather than the activated methylene group.

The ^{13}C−T_1 values of trehalose were also measured to identify the interacting sites in the sugar. As shown in Table 3, the ^{13}C−

TABLE 2: Effect of Saccharide on the Spin−Lattice Relaxation Time (T_1) of Dienes

	spin−lattice relaxation time T_1/s[a]					
	1,3-butadiene	1,3-pentadiene	1,4-pentadiene		2,5-heptadiene	
	cis-olefin H-1,6	*cis*-olefin H-1,3	*cis*-olefin H-1,3,6,8	activated methylene H-4,5	*cis*-olefin H-2,3,6,7	activated methylene H-4,5
none	6.28	6.28	4.80	3.73	3.81	2.77
	6.14	6.14	4.53	3.69	3.52	2.69
trehalose	5.72	5.72	3.95	3.23	2.84	2.20
	5.09	5.09	3.74	3.05	2.60	1.98
neotrehalose	6.21	6.21	4.66	3.78	3.68	2.77
	6.19	6.19	4.43	3.77	3.53	2.28
nigerose	6.31	6.31	4.77	3.71	3.72	2.71
	6.18	6.18	4.52	3.78	3.51	2.78
kojibiose	6.23	6.23	4.79	3.86	3.77	2.88
	6.37	6.37	4.51	3.67	3.60	2.67
maltose	6.24	6.24	4.78	3.65	3.79	2.66
	6.35	6.35	4.21	3.58	3.21	2.64
isomaltose	6.29	6.29	4.76	3.60	3.74	2.60
	6.34	6.34	4.60	3.55	3.56	2.55
sucrose	6.33	6.33	4.79	3.71	3.79	2.70
	6.32	6.32	4.33	3.52	3.33	2.53
maltitol	6.30	6.30	4.56	3.77	3.54	2.76
	6.32	6.32	4.41	3.61	3.42	2.66
sorbitol	6.28	6.28	4.68	3.72	3.70	2.74
	6.31	6.31	4.47	3.52	3.47	2.55

[a] The T_1 measurements were performed at the molar ratio of saccharide/diene = 2:1.

TABLE 3: Effect of Trehalose on the Chemical Shifts and the Spin−Lattice Relaxation Time (T_1) of 1,4-Pentadiene Carbons

	chemical shifts/ppm		spin−lattice relaxation time T_1/s[a]	
	without rehalose	with trehalose	without trehalose	with trehalose
C-2,4	137.32	136.60	6.76	5.99
C-1,5	115.59	115.00	7.19	5.79
C-3	38.54	38.50	6.11	6.28

[a] The T_1 measurements were performed at the molar ratio of trehalose/1,4-pentadiene = 2:1.

T_1 values of trehalose exhibited marked changes when it was mixed with 1,4-pentadiene. In particular, the $^{13}C-T_1$ values of the C-3,3′and C-6,6′ were markedly decreased, while the T_1 changes of the C-1,1′ and C-2,2′ were very small. It is thought that the large decrease in $^{13}C-T_1$ value of the C-3,3′ and C-6,6′ reflects the lowering of mobility at these carbon sites, probably arising from the interaction between the OH-3 (OH-3′) and OH-6 (OH-6′) hydroxyl groups and the diene. Thus, it is inferred that the OH-3,3′ and OH-6,6′ groups of trehalose mainly participate in the interaction with the 1,4-pentadiene.

To support the results from the above ^{1}H- and ^{13}C NMR experiments, we measured the $^1H-^1H$ NOESY spectrum of a mixture of trehalose and 1,4-pentadiene (molar ratio of 2:1). As can be seen from Figure 3, clear cross peaks were observed between the H-1,8 (5.0 ppm) and H-3,6 (5.4−5.8 ppm) *cis*-olefin proton signals of 1,4-pentadiene and the 3 (or 3′) and 6 (or 6′) methylene proton signals (3.8 ppm) of trehalose. In paper 1, we failed to detect a clear cross peak between the C-3 (or C-3′) methyne proton of trehalose and the *cis*-olefin protons of linoleic acid, although the identification of the interaction site was successfully done using 1D NOE experiments. In this regard, Figure 3 is the first direct evidence for the occurrence of the multiple interaction between the 3 (3′) and 6 (6′) sites of trehalose and the *cis*-olefin double bond.

Computational Analysis for the Trehalose/Diene Complexation. To understand the molecular details of the above trehalose/diene interactions, we first examined a trehalose/2-butene complex. In paper 1, we have already found that OH···π and CH···O interactions are responsible for the complexation of trehalose with a *cis*-olefin double bond of an UFA. Here, on the basis of this information, two kinds of initial structures, differing in the orientation of the sugar to the double bond, were constructed for the trehalose/2-butene complex. The first model (hereafter called model A) is that the OH-3 and OH-6′ are binding to a methylene CH group and the π-bond, respectively. In the second model (hereafter called model B), instead of the OH-3, the OH-2 is binding to the CH group. Model B has been already investigated in paper 1. In general, final optimized energy of a molecule depends on the initial

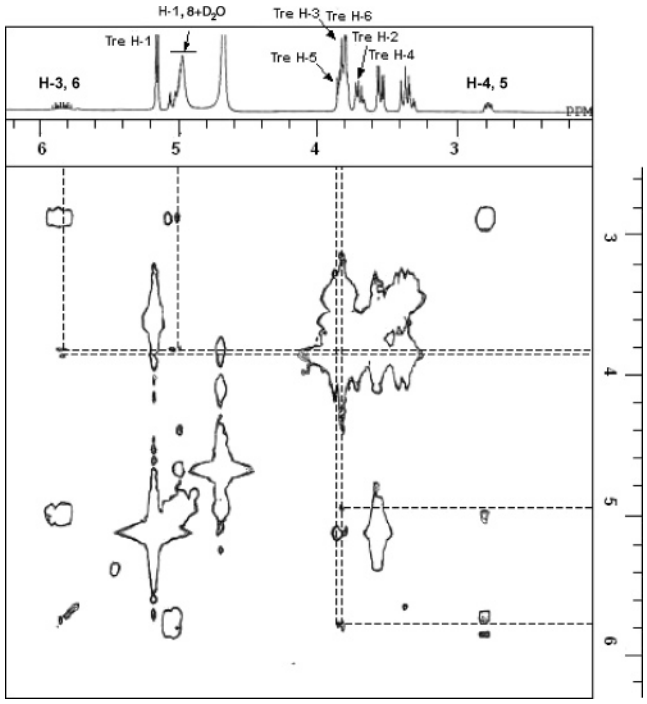

Figure 3. $^1H-^1H$ NOESY spectrum of a mixture of trehalose and 1,4-pentadiene (molar ratio = 2:1).

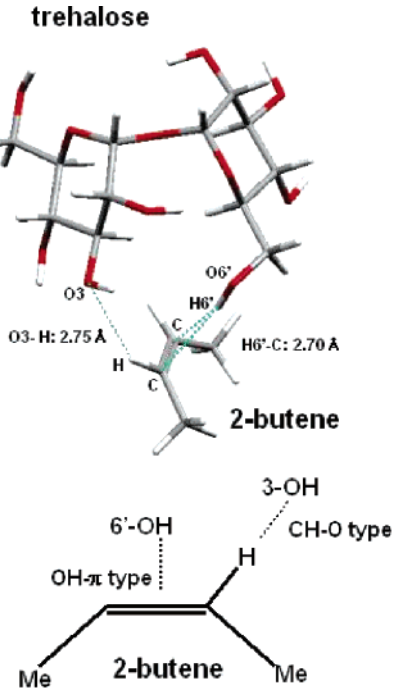

Figure 4. Optimized structures of the trehalose/2-butene complex obtained from the HF/6-31G** calculation. For the isolated trehalose, the torsion angles around the O5′−C5′−C6′−O6′ and C5′−C6′−O6′−H6′ bonds were −30.6° and −47.2°, respectively. The values of these torsion angles were changed upon complexation with 2-butene; namely, the O5′−C5′−C6′−O6′ and C5′−C6′−O6′−H6′ torsion angles were 67.8° and 91.5°, respectively.

conformation assumed. The conformation of trehalose has been extensively studied experimentally[22−26] and theoretically.[27−33] In this study, for both models A and B, the backbone conformation of trehalose was taken from a solution structure determined by a NMR study;[24] namely, the φ (H1−C1−O1−C1′) and ψ (H1′−C1′−O1−C1) angles of the glycosidic bond both were assumed to be −41°. The initial atomic coordinates of model A were first obtained with the aid of MM2 molecular mechanics calculations,[17] followed by energy minimization using the semiempirical PM3 level of calculation.[18] Furthermore, the resultant structure was optimized using the HF/6-31G** or B3LYP/6-31G** level of calculation.

Figure 4 shows the optimized structure of model A, where both the OH···π and the CH···O bonds are stably formed at the OH-6′ and OH-3 sites of trehalose and the backbone conformation of the sugar is different from that of the isolated state. For the isolated trehalose, the ab initio HF/6-31G** calculation gave the optimized φ and ψ angles of −47.2° and −50.4°, respectively, but after the complexation their values were 44.2° and −29.2°. The torsion angles around the O5−C1−O1−C1′ and O5′−C1′−O1−C1 bonds were 70.0° and 62.6° in the isolated state, respectively, and 158.8° and 88.2° in the complexed state. Similar results were obtained from the B3LYP/6-31G** calculation. Therefore, the complexation caused significant conformational changes around the glycosidic bond, especially around the angle φ. This is in contrast to the case of model B, where the changes of the φ and ψ angles were about 2−3° before and after the complexation (Figure 8b in ref 16).

The complex formation energy (or stabilization energy) was obtained as follows

$$\Delta E_{\text{complex}} = E(\text{complex}) - E(\text{trehalose}) - E(\text{2-butene})$$

where the first, second, and third terms on the right-hand side

TABLE 4: Changes in the Spin−Lattice Relaxation Time (T_1) of the Trehalose Carbons Induced by Addition of 1,4-Pentadiene

	chemical shifts/ppm	spin−lattice relaxation time T_1/s[a]	
		without diene	with diene
C-1,1′	94.5	424.1	400.6
C-3,3′	74.1	362.4	300.3
C-2,2′	73.4	342.7	331.0
C-5,5′	72.8	332.3	380.4
C-4,4′	71.5	347.1	349.2
C-6,6′	62.2	235.4	210.5

[a] The T_1measurements were performed at the molar ratio of trehalose/1,4-pentadiene = 2:1.

are the total energies of the complex, trehalose (or methanol), and 2-butene, respectively, and these energies were obtained for the optimized structure of each molecular species. The energy of each species was obtained by five different levels of calculation. The resulting energy data are summarized in Table 5. Irrespective of the theoretical levels used, the complexation energies $\Delta E_{\text{complex}}$ for models A and B have substantially negative values, indicating the formation of a stable intermolecular complex. Interestingly, for both interaction models, the $\Delta E_{\text{complex}}$ values from the B3LYP/6-31G**//B3LYP/6-31G** and MP2/6-31G**//HF/6-31G** calculations are considerably smaller than that from the HF/6-31G**//HF/6-31G** calculation, while the B3LYP/6-31G** and MP2/6-31G** results are numerically close to each other. This indicates that the electron correlation effect significantly contributes to stabilization of the intermolecular complexes. The effect of basis set superposition errors (BSSE) was analyzed using the following two approaches. First, the well-known counterpoise (CP) correction[34] was applied to the HF/6-31G**//HF/6-31G** and B3LYP/6-31G**//B3LYP/6-31G** results. Second, we performed larger basis set calculations, namely, the HF/6-311++G** or B3LYP/6-311++G** level, by which most BSSE errors might be avoided. With the BSSE correction, the $\Delta E_{\text{complex}}$ value significantly increases irrespective of both the theoretical levels and the correction methods used. In addition, for each interaction model, the CP-corrected energies agree with those from the large basis set calculations within ±1 kcal mol^{-1}. For example, the CP-corrected energy (−6.03 kcal mol^{-1}) for the B3LYP/6-31G** result of model A is close to that (−5.28 kcal mol^{-1}) from the B3LYP/6-311++G** calculation. One of the most interesting findings from Table 5 is that model A undergoes the electron correlation effect more largely than model B, leading to a larger stabilization of model A (see the results from the B3LYP/6-31G** and MP2/6-31G** calculations). Taken together with the results of the BSSE correction, the stabilization energy of model A is evaluated to be 5−6 kcal mol^{-1}, while that of model B is <5 kcal mol^{-1}.

Next, we examined a more realistic model corresponding to the above NMR experiments, that is, trehalose/heptadiene = 2:1 complex. The initial structures were constructed in a similar way to the case of the trehalose/2-butene complex and finally optimized by the HF/6-31G** or B3LYP/6-31G** calculation. Figure 5 depicts the most stable complex obtained, where each of the two trehalose molecules binds to one of the double bonds in a fashion similar to that in model A of the trehalose/2-butene complex. As described above, the B3LYP/6-31G** and MP2/6-31G** calculations tend to provide similar numerical results, which indicates that the less time-consuming calculation; that is, the B3LYP calculation, is sufficiently accurate for the present purpose. Thus, the MP2 calculation was omitted for the trehalose/heptadiene complex. The stabilization energies from

TABLE 5: Energies of the Trehalose/2-Butene Complex

methods	2-butene/au	trehalose/au	complex/au		$\Delta E_{complex}$/kcal mol^{-1}	
			model A[a]	model B[b]	model A[a]	model B[b]
HF/6-31G**//HF/6-31G**	−156.1180	−1290.7220	−1446.8465	−1446.8489	−4.03 (−1.83)[c]	−5.52 (−3.41)[c]
B3LYP/6-31G**//B3LYP/6-31G**	−157.2332	−1297.9509	−1455.2018	−1455.1966	−11.04 (−6.03)[c]	−7.78 (−4.49)[c]
MP2/6-31G**//HF/6-31G**	−156.6851	−1294.3550	−1451.0574	−1451.0543	−10.87	−8.91
HF/6-311++G**//HF/6-31G**	−156.1470	−1291.0629	−1447.2131	−1447.2165	−2.00	−4.17
B3LYP/6311++G**//B3LYP/6-31G**	−157.2694	−1298.3441	−1455.6219	−1455.6215	−5.28	−5.05

[a] This study. [b] The previous study (ref 16). [c] The energies after the BSSE correction.

TABLE 6: Energies for the Trehalose/Heptadiene Complex

methods	heptadiene/au	trehalose/au	complex/au	$\Delta E_{complex}$/kcal mol^{-1}
RHF/6-31G**	−272.0406	−1290.7220	−2853.5062	−13.55 (−9.25)[a]
B3LYP/6-31G**	−279.9496	−1297.9509	−2875.8742	−14.28 (−11.06)[a]

[a] The energies after the BSSE correction are shown in the parentheses.

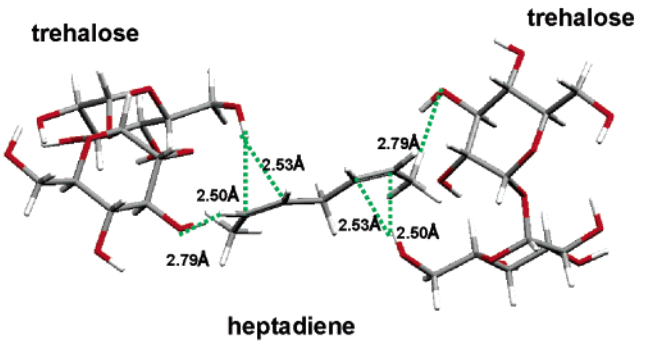

Figure 5. HF/6-31G**-optimized structure of the trehalose/pentadiene complex.

the HF/6-31G** or B3LYP/6-31G** calculations were −13.55 and −14.28 kcal mol^{-1} before the BSSE correction and −9.25 and −11.06 kcal mol^{-1} after the correction, respectively (Table 6). These results strongly support the formation of the trehalose/heptadiene complex with 2:1 stoichiometry, consistent with the present NMR studies.

Activation Energy of the Hydrogen Abstraction Reaction. As described in the Introduction, one of the purposes of this study is to theoretically analyze the depression effect of trehalose on the following hydrogen abstraction reaction of an UFA[10]

$$-CH_2-CH=CH-CH_2-CH=CH-CH_2- \rightarrow -CH_2-CH=CH-\overset{\bullet}{C}H-CH=CH-CH_2- \quad (1)$$

The essential part of the reactant could be modeled by heptadiene, and hence the trehalose/heptadiene complex shown in Figure 5 is a better model for the above purpose. However, in paper 1, alternative simpler model systems were used to examine the effect of trehalose on the same reaction. Namely, two model systems shown in Figure 6 were constructed: the former has two methanol molecules binding to the two π systems of heptadiene through the OH$\cdots\pi$ type interaction and the latter has four methanol molecules binding to the four CH groups through the CH$\cdots$O type hydrogen bond. In what follows, we compare the results based on the above three models.

First, we analyzed the simple hydrogen abstraction reaction that spontaneously occurs without any initiator such as a methyl radical. While the reaction has already been studied for the methanol/heptadiene complex (Figure 6) in paper 1, here the energy profile of the reaction was newly obtained for the

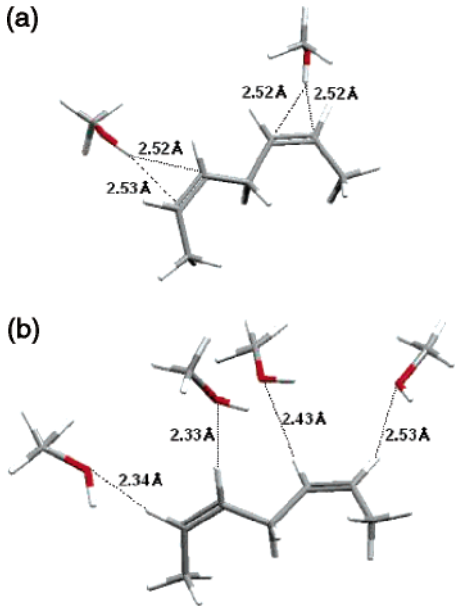

Figure 6. HF/6-31G**-optimized structure of the methanol/heptadiene complex showing the (a) OH$\cdots\pi$ interaction model and the (b) CH$\cdots$O interaction model.

trehalose/heptadiene complex shown in Figure 5. The energies of the reactant, transition state (TS), and product were evaluated using the UB3LYP/6-31G** or UHF/6-31G** method. The results are summarized in Table 7. Irrespective of the methods used, the activation energy for hydrogen abstraction is significantly increased by the occurrence of interaction with trehalose, namely, from 111.06 to 121.86 kcal mol^{-1} (UHF/6-31G**) and from 86.03 to 95.88 kcal mol^{-1} (UB3LYP/6-31G**). Consequently, the activation energy difference, obtained by subtracting the value in the isolated state from that in the complex state, is 10.76 kcal mol^{-1} (UHF) and 9.87 kcal mol^{-1} (UB3LYP). It is of interest to compare these results with those for the two methanol/heptadiene complexes, whose data were cited in Table 7. As already pointed out in paper 1, the activation energy increase on going from the isolated to complexed state is larger in the OH$\cdots\pi$ model (Figure 6a) than that in the CH$\cdots$O one (Figure 6b), despite the fact that the number of the total hydrogen bonds is smaller in the former than that in the latter. In addition, the activation energy increase for the OH$\cdots\pi$ model is nearly equal to that for the trehalose/heptadiene complex regardless of the computational methods used, for example, 10.86 kcal mol^{-1} (OH$\cdots\pi$) and 1.76 kcal mol^{-1} (trehalose) for

TABLE 7: Calculated Results for the Hydrogen Abstraction Reaction (Hydrogen Breaking Model) of Heptadiene, Heptadiene/Methanol, and Heptadiene/Trehalose Complexes

methods	models	reactant/au	transition state/au	product/au	activation energy/ kcal mol^{-1}	activation energy difference/kcal mol^{-1}
UHF/6-31G**	heptadiene[a]	−272.0344	−271.8574	−271.4532	111.06	
	MeOH (CH···O)[b]	−732.2361	−732.0436	−731.6133	120.79	9.68
	MeOH (OH···π)[c]	−502.1411	−501.9467	−501.5317	121.99	10.86
	trehalose[d]	−2853.5062	−2853.3120	−2852.7071	121.86	10.76
UB3LYP/6-31G**	heptadiene[a]	−273.9436	−273.8066	−273.4050	86.03	
	MeOH (CH···O)[b]	−736.8617	−736.7146	−736.1906	92.31	6.49
	MeOH (OH···π)[c]	−505.4059	−505.2517	−504.7224	96.76	9.76
	trehalose[d]	−2875.8742	−2875.7214	−2875.0620	95.88	9.87

[a] Isolated heptadiene. [b] Model shown in Figure 6b. [c] Model shown in Figure 6a. [d] Model shown in Figure 5.

TABLE 8: Electron Densities on the Heptadiene Carbon Atoms[e]

	Mulliken charges						
	C1	C2	C3	C4	C5	C6	C7
			RHF/6-31G**				
heptadiene[a]	−0.358	−0.128	−0.119	−0.277	−0.119	−0.128	−0.359
MeOH (CH···O)[b]	−0.366	−0.183	−0.130	−0.254	−0.170	−0.160	−0.366
MeOH (OH···π)[c]	−0.369	−0.160	−0.151	−0.255	−0.155	−0.156	−0.369
trehalose[d]	−0.382	−0.182	−0.176	−0.209	−0.177	−0.182	−0.377
			B3LYP/6-31G**				
heptadiene[a]	−0.352	−0.134	−0.112	−0.276	−0.112	−0.134	−0.352
MeOH (CH···O)[b]	−0.358	−0.146	−0.126	−0.268	−0.128	−0.144	−0.356
MeOH (OH···π)[c]	−0.357	−0.158	−0.160	−0.253	−0.170	−0.156	−0.356
trehalose[d]	−0.367	−0.174	−0.197	−0.205	−0.197	−0.175	−0.365

[a] Isolated heptadiene. [b] Model shown in Figure 6b. [c] Model shown in Figure 6a. [d] Model shown in Figure 5. [e] Heptadiene: $H_3C^1-C^2H=C^3H-C^4H_2-C^5H=C^6H-C^7H_3$.

the UHF/6-31G** calculation. Therefore, it was concluded that the OH···π interaction is more effective for lowering the reactivity of the activated methylene group.

To interpret the above results, we examined the charge distribution on the heptadiene molecule, and the results are summarized in Table 8, where electron densities were calculated by Mulliken population analysis. The activated methylene carbon (C4) of free heptadiene has a relatively large negative charge. However, when accompanied by the hydrogen bond formation between the double bonds and trehalose or methanol, the negative charge on C4 is greatly decreased, and simultaneously the other carbon atoms become more negatively charged. This finding indicates that the electron on the activated methylene is delocalized toward the π-bonds and additionally a significant amount of charge transfer occurs from the ligand (trehalose or methanol) to the π-bonds. Such a charge rearrangement is more remarkable in the trehalose/heptadiene complex than that in the two types of trehalose/methanol ones, suggesting that the OH···π and CH···O multiple hydrogen bonds can more strongly affect the electronic state of the double bond. The decrease in electron density on C4 is expected to lower the activity of the C4 methylene group, hence leading to depression of the hydrogen abstraction reaction.

Next, we carried out the intrinsic reaction coordinate (IRC) calculation for the hydrogen abstraction reaction initiated by methyl radical. The carbon atom of the methyl radical was coordinated along the C−H bond vector of the active methylene hydrogen of heptadiene. The distance between the active methylene hydrogen and the methyl radical carbon were changed in 0.1 Å intervals from 1.1 to 2.4 Å, and the minimum energy path calculation for C−H bond breaking was carried out. The maximal energy structure, located nearly around the transition state, was picked out, and the transition state was searched using the UHF/6-31G** or UB3LYP/6-31G** level of calculation. These IRC and TS calculations were carried out for an isolated heptadiene/methyl radical system, methanol/heptadiene/methyl radical, and trehalose/heptadiene/methyl radical systems. The TS structure of the trehalose/heptadiene/methyl radical system is shown in Figure 7, and the activation energies for all of the systems studied are summarized in Table 9. For the isolated heptadiene/methyl radical, the activation energies were 14.81 kcal mol^{-1} (UHF/6-31G**) and 9.22 kcal mol^{-1} (UB3LYP/6-31G**). Those for the methanol/heptadiene/methyl radical systems were 21.52 kcal mol^{-1} (UHF) and 22.15 kcal mol^{-1} (UB3LYP) for the CH···O interaction model and 26.98 kcal mol^{-1} (UHF) and 27.61 kcal mol^{-1} (UB3LYP) for the OH···π interaction model. For the trehalose/heptadiene/methyl radical

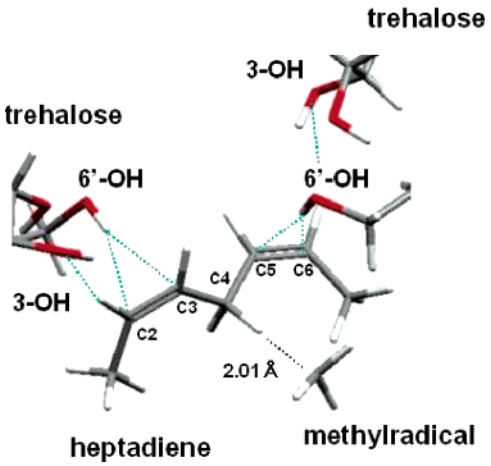

Figure 7. Transition state of the trehalose/heptadiene 2:1 complex in the methyl-radical-induced reaction (CH_2···CH_3 distance of 2.01 Å) obtained from the UHF/6-31G** calculations. The structures of the trehalose molecules are truncated. The values of the C2−C3−C4−C5 and C6−C5−O4−C3 torsion angles deviated from the planar trans structure; namely, the C2−C3−C4−C5 and C6−C5−O4−C3 torsion angles were 157.93° and 150.44°, respectively.

TABLE 9: Calculated Results for the Hydrogen Abstraction Reaction (Methyl Radical Model) of the Heptadiene, Heptadiene/Methanol, and Heptadiene/Trehalose Complexes

methods	models	reactant/au	transition state/au	product/au	activation energy/ kcal mol^{-1}	activation energy difference/kcal mol^{-1}
UHF/6-31G**	heptadiene[a]	−311.6027	−311.5791	−311.6581	14.81	
	MeOH (CH···O)[b]	−756.5413	−756.5070	−756.5970	21.52	6.70
	MeOH (OH···π)[c]	−534.9390	−534.8960	−535.0177	26.98	12.17
	trehalose[d]	−2892.9355	−2892.8754	−2892.9651	37.78	22.93
UB3LYP/6-31G**	heptadiene[a]	−313.7885	−313.7738	−313.8780	9.22	
	MeOH (CH···O)[b]	−762.0380	−762.0027	−762.1050	22.15	12.95
	MeOH (OH···π)[c]	−541.6940	−541.6500	−541.7640	27.61	18.36
	trehalose[d]	−2909.7309	−2909.6693	−2909.7499	38.65	29.45

[a] Isolated heptadiene. [b] Model shown in Figure 6b. [c] Model shown in Figure 6a. [d] Model shown in Figure 5.

system, the activation energy was further increased, namely, 37.78 kcal mol^{-1} (UHF) and 38.65 kcal mol^{-1} (UB3LYP). These results indicate that the OH···π and CH···O multiple hydrogen bonds can more strongly affect the electronic state of the diene, consistent with the tendency of the electronic distribution (Table 7). Therefore, it can be concluded that the hydrogen abstraction reaction 1 is significantly depressed by the interaction with trehalose.

Discussion

As described in the Introduction, the aim of this work was to address the following issues: (1) whether trehalose generally binds to *cis*-olefin double bonds other than those of UFAs, (2) establishment of an interaction model acceptable from both the experimental and the theoretical viewpoints, and (3) to what extent trehalose depresses methyl-radical-induced oxidation of an UFA. To experimentally find the answers to the first issue, we selected several diene compounds including conjugated dienes (1,3-butadiene and 1,3-pentadiene) and nonconjugated dienes (1,4-pentadiene and 2,5-heptadiene), the latter of which is also regarded as a minimal model of an UFA because it possesses an activated methylene group.

The comparison of the ^{1}H−T_1 results for the five different trehalose/diene mixtures clearly indicated that this sugar selectively interacts with the *cis*-olefin hydrogen pair (cis double bond) of the partner diene and the stoichiometry of the resulting complex is 2:1 (trehalose/diene). In addition, the ^{13}C−T_1 and ^{1}H−^{1}H NOESY results revealed that the sites of trehalose responsible for the interaction are the C-3 (C-3′) and C-6 (C-6′) hydroxyl groups. These results are consistent with the previous ones for the trehalose/UFA systems.[16] Through combination of these results, it can be concluded that the complex formation between trehalose and a cis double bond is a rather universal phenomenon. In contrast, the other disaccharides studied do not share such a property even in neotrehalose (Table 2). Therefore, a 1,1-α,α-linkage is the structural key to the specific interaction with a cis double bond.

The present quantum chemical calculations revealed that trehalose is able to form a stable intermolecular complex with heptadiene with a 2:1 stoichiometry, and the OH-3 (OH-3′) and OH-6′ (OH-6) groups of each sugar participate in multiple hydrogen bonds with one of the cis double bonds. These results are consistent with the present NMR results. It is of interest to examine to what extent the OH-3/OH-6′ multiple bond is more stable than the OH-2/OH-6′ one. However, we did not perform the calculation for the latter model because the calculation for a relatively large size system, composed of two trehalose molecules and heptadiene, is very time-consuming. Instead, we performed careful calculations for the two models (models A and B) of the trehalose/2-butene complex. As described in the previous section, the stabilization energy of model A is larger than that of model B by ∼1 kcal mol^{-1}. Although this difference is not sufficiently large compared with the thermal energy (0.6 kcal mol^{-1}) at room temperature, it was confirmed that the former is a preferentially formed complex.

In the present trehalose/2-butene model, the torsion angles around the O5−C1−O1−C1′ and O5′−C1′−O1−C1 bonds were 158.8° and 88.2°, respectively. The former is closer to trans conformation than gauche. According to a recent quantum chemical study on the intrinsic conformation of trehalose, the global energy minimum occurs in a region where the angles of the O5−C1−O1−C1′ and O5′−C1′−O1−C1 bonds both are 60−80°, corresponding to a gauche conformation.[30] And various experimental studies,[22−26] including X-ray and NMR analyses, also indicated that these dihedral angles are 60−80° in the crystalline and solution states. Thus, in the complex state, one of the two dihedral angles is largely distorted from the global minimum of the isolated state. As can be seen from Figure 4, such a distortion is necessary for the OH-3 to approach one of the CH groups of a diene double bond. To evaluate the distortion energy, we calculated the energy of the trehalose moiety alone after the geometry of 2-butene was deleted from that of the whole complex (Figure 4). The resulting energy at the HF/6-31G** level was −1290.7190 au. After subtraction of it from the energy (−1290.7220 au) of the isolated trehalose (Table 5), the distortion energy was given to be 1.9 kcal mol^{-1}. Similar results were also obtained for the B3LYP/6-31G** calculation. Although this value seems to be rather small, it is confirmed to be reasonable by reference to conformational energy maps given in ref 30. Regardless of the theoretical levels used, the potential energy well of trehalose is considerably shallow and broad. As a result, either $\phi_{O5-C1-O1-C1'}$ or $\phi_{O5'-C1V-O1-C1}$ is allowed to be near 160° when the other stays around 60°−80° (Figure 4a in ref 30). Thus, the trehalose conformation in Figure 4 corresponds to that located on the border of the potential well for the isolated state. The above distortion energy is sufficiently compensated for by the interaction with 2-butene, resulting in the formation of the stable complex (Figure 4). As described in the previous section, the electron correlation effect is a main contributor for the stabilization.

Formation of the above multiple hydrogen bond is entropically more favorable than the physical process where a couple of solvent molecules (water or methanol) are arranged to form similar multiple interactions with a double bond. Thus, it is expected that trehalose would preferentially bind to the double bond instead of solvent molecules when its concentration is beyond a threshold value. Once the multiple interaction is formed, it would be kept with a substantial lifetime because the free rotations around the glycosicic bonds are not allowed as evident from the conformational energy map.[30] Another unique property to be noted is that trehalose does not form interresidue, intramolecular hydrogen bonds that are often found

for other disaccharides such as maltose and sucrose. The interresidue bonds in maltose and sucrose might discourage the type of interaction proposed in Figure 4, but the hydroxyl groups of trehalose are open for intermolecular interactions.

Finally, we discuss the antioxidative activity of trehalose. According to the analysis of the simple hydrogen abstraction reaction from the activated methylene group of heptadiene, the multiple interactions with trehalose cause an increase of ca. 10 kcal mol^{-1} in the activation energy irrespective of the computational methods used (Table 7). This is consistent with the results predicted from the more simple interaction models (Figure 6, parts a and b). However, as understood from the activation energy (86 or 111 kcal mol^{-1}) for the free heptadiene, the simple hydrogen abstraction reaction would not spontaneously occur under normal conditions, and hence it might not be a better model for the actual reactions examined in our experimental work.[12] Usually, the peroxidation of an UFA is initiated by heat or radical species.[10] In fact, our present calculation indicated that the activation energy for the free heptadiene was dramatically lowered to 9 kcal mol^{-1} (UB3LYP) or 14 kcal mol^{-1} (HF) when the reaction was assumed to be initiated by methyl radical. Thus, this reaction is regarded as a more realistic model. As can be seen from Table 9, on complexation with trehalose, the activation energy increases by ca. 30 kcal mol^{-1} (UB3LYP) and ca. 23 kcal mol^{-1} (UHF). Interestingly, the multiple site interaction with trehalose elevates the activation energy more largely (10 kcal mol^{-1}) than that of the CH$\cdots$O or OH$\cdots\pi$ interaction with methanol. The increase of the activation energy corresponds to the lowering of the chemical activity of the methylene group of interest. As described in the previous section, such an activity lowering is well correlated with the degree of a decrease in the negative charge on C4. Therefore, the antioxidant activity of trehalose was successfully accounted for from viewpoints of both energetics and electronic structure.

It has been demonstrated that several other disaccharides, such as sucrose, maltose, and neotrehalose, show negligible effect on the peroxidation.[12] Through combination of this study with paper 1, it is evident that those disaccharides cannot interact directly with oxidation-sensitive parts of an UFA and hence cannot modify the oxidation reaction.

In conclusion, the present study provided the satisfactory answers to all of the issues to be addressed. The finding that trehalose can form an intermolecular complex with various cis double bonds makes us expect that this sugar can also interact with benzene compounds, whose double bonds are cis rather than trans. This interesting issue is under investigation now in our laboratory. Finally, it should be stressed that the uniqueness of trehalose comes from the presence of an α,α-1,1-linkage.

Acknowledgment. This work was supported in part by the Program for Promotion of Basic Research Activities for Innovative Biosciences (PROBRAIN) and Grants-in-Aid for Scientific Research on Priority Areas (no. 16041212) from the Ministry of Education, Culture, Sports, Science and Technology of Japan. We thank the Computer Center, Institute for Molecular Science, Okazaki, Japan, for the use of the supercomputer system and the Computer Center, Tokyo Institute of Technology, Japan, for the use of the SGI Origin 2000 system.

References and Notes

(1) Elbein, A. D. *Adv. Carbohydr. Chem. Biochem.* **1974**, *30*, 227.
(2) Chaen, H. *J. Appl. Glycosci.* **1997**, *44*, 115.
(3) Kubota, M.; Sawatani, I.; Oku, K.; Takeuchi, K.; Murai, S. *J. Appl. Glycosci.* **2004**, *51*, 63.
(4) Laere, A. V. *FEMS Microbiol. Rev.* **1989**, *63*, 201.
(5) Singer, M. A.; Lindquist, S. *TIBTECH* **1998**, *16*, 460.
(6) Argüelles, J. C. *Arch. Microbiol.* **2000**, *174*, 217.
(7) Crowe, J. H.; Crowe, L. M.; Carpenter, J. F.; Wistrom, C. A. *Biochem. J.* **1987**, *242*, 1.
(8) Crowe, J. H.; Crowe, L. M.; Carpenter, J. F.; Rudolph, A. S.; Wistrom, C. A.; Spargo, B. J.; Anchordoguy, T. J. *Biochim. Biophys. Acta* **1988**, *947*, 367.
(9) Crowe, J. H.; Carpenter, J. F.; Crowe, L. M. *Annu. Rev. Physiol.* **1998**, *60* (7), 73.
(10) Niki, E. *J. Oleo Sci.* **2001**, *50*, 313.
(11) Oku, K.; Chaen, H.; Fukuda, S.; Kurimoto, M. *Nippon Shokuhin Kagaku Kougaku Kaishi* **1999**, *46*, 749.
(12) Oku, K.; Kurose, M.; Kubota, M.; Fukuda, S.; Kurimoto, M.; Tujisaka, Y.; Sakurai, M. *Nippon Shokuhin Kagaku Kougaku Kaishi* **2003**, *50*, 133.
(13) Benaroudj, N.; Lee, D. H.; Goldberg, L. A. *J. Biol. Chem.* **2001**, *276*, 24261.
(14) Terao, J. *J. Oleo Sci.* **2001**, *50*, 393.
(15) Burkitt, M. J.; Gilbert, B. C. *Free Radical Res.* **1999**, *10*, 265.
(16) Oku, K.; Watanabe, H.; Kubota, M.; Fukuda. S.; Kurimoto, M.; Tujisaka, Y.; Komori, M.; Inoue, Y.; Sakurai, M. *J. Am. Chem. Soc.* **2003**, *125*, 12739.
(17) Allinger, N. L. *J. Am. Chem. Soc.* **1977**, *99*, 8127.
(18) Stewart, J. J. P. *MOPAC2000*; Fujitu Ltd.: Tokyo, Japan, 1999.
(19) Frisch, M. J.; Trucks, G. W.; Schlegel, H. B.; Scuseria, G. E.; Robb, M. A.; Cheeseman, J. R.; Zakrzewski, V. G.; Montgomery, J. A., Jr.; Stratman, R. E.; Burant, J. C.; Dapprich, S.; Millam, J. M.; Daniels, A. D.; Kudin, K. N.; Strain, M. C.; Farkas, O.; Tomasi, J.; Barone, V.; Cossi, M.; Cammi, R.; Mennucci, B.; Pomelli, C.; Adamo, C.; Clifford, S.; Ochterski, J.; Petersson, G. A.; Ayala, P. Y.; Cui, Q.; Morokuma, K.; Malick, D. K.; Rabuck, A. D.; Raghavachari, K.; Foresman, J. B.; Cioslowski, J.; Ortiz, J.; Stefanov, B. B.; Liu, G.; Liashenko, A.; Piskorz, P.; Komaromi, I.; Gomperts, R.; Martin, R. L.; Fox, D. J.; Keith, T.; Al-Laham, M. A.; Peng, C. Y.; Nanayakkara, A.; Gonzalez, C.; Challacombe, M.; Gill, P. M. W.; Johnson, B. G.; Chen, W.; Wong, M. W.; Andres, J. L.; Head-Gordon, M.; Replogle, E. S.; Pople, J. A. *Gaussian 98*; Gaussian Inc.: Pittsburgh, PA, 1998.
(20) Bloembergen, N.; Purcell, E. M.; Pound, R. V. *Phys. Rev.* **1948**, *73*, 679.
(21) Farrar, T. C.; Becker, E. D. *Pulse and Fourier Transform NMR, Introduction to Theory and Methods*; Academic Press: New York, 1971; Chapter 4.
(22) Brown, G. M.; Tohrer, D. C.; Berking, B.; Beevers, C. A.; Gould, R. O.; Simpson, R. *Acta Crystallogr.* **1972**, *B28*, 3145.
(23) Taga, T.; Senma, M.; Osaki, K. *Acta Crystallogr.* **1972**, *B28*, 3258.
(24) Batta, G. J.; Kövér, K. E.; Gervay, J.; Hornyäk, M.; Roberts, G. M. *J. Am. Chem. Soc.* **1997**, *119*, 1336.
(25) Duda, C. A.; Stevens, E. S. *J. Am. Chem. Soc.* **1990**, *112*, 7406.
(26) Tvaroška, I.; Václavík, L. *Carbohydr. Res.* **1987**, *160*, 137.
(27) Dowd, M. K.; Reilly, P. J.; French, A. D. *J. Comput. Chem.* **1992**, *13*, 102.
(28) Liu, Q.; Schmidt, R. K.; Teo, B.; Karplus, P. A.; Brady, J. W. *J. Am. Chem. Soc.* **1997**, *119*, 7851.
(29) Engelsen, S. B.; Pérez, S. J. *J. Phys. Chem. B* **2000**, *104*, 9301.
(30) French, A. D.; Johnson, G. P.; Kelterer, A.-M.; Dowd, M. K.; Cramer, C. J. *J. Phys. Chem. A* **2002**, *106*, 4988.
(31) Brandl, M.; Weiss, M. S.; Jabs, A.; Sühnel, J.; Hilgenfeld, R. *J. Mol. Biol.* **2001**, *307*, 357.
(32) Xantheas, S. S.; Dunning, T. H. *J. Chem. Phys.* **1993**, *99*, 8774.
(33) Xantheas, S. S. J. Chem. Phys. **1994**, 100, 7523; Xantheas, S. S. *J. Chem. Phys.* **1995**, *102*, 4505.
(34) van Duijneveldt, F. B.; van Duijneveldt-van de Rijdt, J. G. C. M.; van Lenthe, J. H. *Chem. Rev.* **1994**, *94*, 1873.